AAEC/E360

AUSTRALIAN ATOMIC ENERGY COMMISSION

RESEARCH ESTABLISHMENT

LUCAS HEIGHTS

THE EIGENVALUES OF THE DISCRETE ORDINATES EQUATIONS IN SLAB GEOMETRY

by

I. J. DONNELLY

September 1975

ISBN 642 99691 1

AUSTRALIAN ATOMIC ENERGY COMMISSION

RESEARCH ESTABLISHMENT

LUCAS HEIGHTS

THE EIGENVALUES OF THE DISCRETE ORDINATES EQUATIONS IN SLAB GEOMETRY

by

I. J. DONNELLY

ABSTRACT

The discrete ordinates approximation of the one–group, source–free, neutron transport equation has been solved analytically for slab geometry. The resulting eigenvalues are functions of both the angular quadrature and the spatial mesh used in the discrete ordinates equations. The dependence of the eigenvalues on the angular quadrature has been examined for the three limiting cases of $c << 1$, $|1-c| << 1$ and $c >> 1$, where $c = \sigma_s/\sigma_t$. Both the diamond difference and step function approximations have been considered in the evaluation of the eigenvalue dependence on the spatial mesh size. When the neutron flux is well described by a function of the form $\exp(-\kappa x)$, the diamond difference approximation gives an eigenvalue $\kappa^d \simeq \kappa(1 + (\kappa\Delta)^2/12)$, where κ is the eigenvalue for small values of the mesh size Δ, while the step function approximation gives an eigenvalue $\kappa^s \simeq \kappa(1-0.4\,\sigma_t\,\Delta)$.

National Library of Australia card number and ISBN 642 99691 1

The following descriptors have been selected from the INIS Thesaurus to describe the subject content of this report for information retrieval purposes. For further details please refer to IAEA–INIS–12 (INIS: Manual for Indexing) and IAEA–INIS–13 (INIS: Thesaurus) published in Vienna by the International Atomic Energy Agency.

ANALYTICAL SOLUTION; ANISOTROPY; DISCRETE ORDINATE METHOD; EIGEN VALUES; GEOMETRY; MULTI GROUP THEORY; NEUTRON FLUX; NEUTRON TRANSPORT THEORY; SCATTERING; SLABS

CONTENTS

1. INTRODUCTION

The neutron transport equation is commonly solved numerically by use of the discrete ordinates (S_N) approximation. In this approximation, the neutron angular flux is evaluated for discrete directions and at discrete spatial points. This gives a flux solution which is dependent upon the angular and spatial mesh used, but which becomes exact for infinitesimal mesh sizes. The usual method of estimating the error for a calculation using a given mesh is to recalculate using smaller mesh sizes and note the changes in flux. This is often impractical for calculations involving large numbers of mesh points, so an *a priori* criterion for evaluation of the accuracy of a given calculation would be useful. With this in mind, the discrete ordinates form of the one-group, time-independent, source-free neutron transport equation has been solved analytically in slab geometry.

An analysis has been made of the dependence of the resulting eigenvalues and their corresponding eigenfunctions on the angular quadrature and spatial mesh size used in the discrete ordinates equations. This treatment illustrates the rate of convergence of the discrete ordinates approximate solution of the transport equation as angular and spatial mesh sizes decrease. Particular attention has been paid to the behaviour of the dominant eigenvalue which determines the flux values in large homogeneous systems such as radiation shields.

The dependence of the eigenvalues on the angular quadrature is considered in Section 2. The effect of spatial mesh size is evaluated in Section 3 assuming the diamond difference form of flux averaging, and in Section 4 assuming the step function form of flux averaging. In Sections 2 to 4 the neutron scattering is assumed to be isotropic. The analysis is repeated allowing anisotropic scattering in Section 5. A brief discussion of the extension of the one-group results to realistic multigroup problems is given in Section 6. In Appendix C an analysis is made of the dependence on spatial mesh size of the eigenvalues of the one-group diffusion theory equation.

2. DISCRETISATION OF THE ANGULAR VARIABLE

The one-group, time-independent, source-free neutron transport equation in slab geometry is

$$\mu \frac{\partial \psi(x,\mu)}{\partial x} + \psi(x,\mu) = \frac{c\phi(x)}{2} , \qquad (1)$$

where $\psi(x,\mu)$ is the angular flux per 2π steradians,

$$\phi(x) = \int_{-1}^{1} \psi(x,\mu)\, d\mu , \qquad (2)$$

$c = \sigma_s / \sigma_t$, and spatial dimensions are expressed in mean free path units.

The discrete ordinates (S_N) method for solution of the transport equation evaluates the angular flux for a set of N direction cosines $\{\mu_m\}$ with associated weights $\{\omega_m\}$. In this report, only symmetric quadrature sets will be used and the direction cosines are ordered so that $\mu_1 > \mu_2 > \ldots > \mu_N$.

Hence

$$\mu_m = -\mu_{N-m+1} \text{ and } \omega_m = \omega_{N-m+1} , \quad m = 1,2,\ldots,N/2 . \qquad (3)$$

Equation (1) is therefore replaced by a set of N coupled differential equations:

$$\mu_m \frac{d\psi_m(x)}{dx} + \psi_m(x) = \frac{c\phi(x)}{2} , \qquad m = 1,2,\ldots,N , \qquad (4)$$

where

$$\psi_m(x) = \psi(x,\mu_m) \quad , \qquad \phi(x) = \sum_{m=1}^{N} \omega_m \psi_m(x) \quad ,$$

and the weights are normalised so that

$$\sum_{m=1}^{N} \omega_m = 2 \quad . \tag{5}$$

Equation (4) may be solved as follows. Replace $\psi_m(x)$ by $\zeta_m e^{\kappa x}$, multiply both sides by $\omega_m/(1 + \mu_m\kappa)$, sum for m = 1 to N and use Equation (3) to obtain the relationship

$$\sum_{m=1}^{N/2} \frac{\omega_m}{1-\mu_m^2\kappa^2} = \frac{1}{c} \quad . \tag{6}$$

This has been obtained previously by Davison (1957). A sketch of the function

$$f(\kappa^2) = \sum_{m=1}^{N/2} \frac{\omega_m}{1-\mu_m^2\kappa^2} \tag{7}$$

is given in Figure 1. From this figure it is apparent that there are N/2 roots for κ^2 in Equation (6). Hence the eigenvalues of Equation (4) are $\pm\kappa_m (m = 1,2,\ldots,N/2)$, with the properties:

(i) $\dfrac{1}{\mu_{m-1}} < \kappa_m \leqslant \dfrac{1}{\mu_m}$, $\quad m = 2,3,\ldots,N/2$;

(ii) $0 \leqslant \kappa_1 \leqslant \dfrac{1}{\mu_1}$, $\quad 1 \geqslant c \geqslant 0$;

(iii) $\kappa_1 = iB_1$ with $B_1 > 0$, $\quad c > 1$. (8)

The general solution for Equation (4) has the form

(i) $\psi_m(x) = \sum_{i=1}^{N/2} F_{m,i}(x)$, $\quad 0 \leqslant c < 1$;

(ii) $\psi_m(x) = \zeta^c_{m,1} + \zeta^s_{m,1} x + \sum_{i=2}^{N/2} F_{m,i}(x)$, $\quad c = 1$;

(iii) $\psi_m(x) = \zeta^c_{m,1} \cos(B_1 x) + \zeta^s_{m,1} \sin(B_1 x) + \sum_{i=2}^{N/2} F_{m,i}(x)$, $\quad c > 1$; (9)

where

$$F_{m,i}(x) = \zeta^c_{m,i} \cosh(\kappa_i x) + \zeta^s_{m,i} \sinh(\kappa_i x) \quad ,$$

and the terms $\zeta^{c,s}_{m,i}$ are constants determined by Equation (4) and by the boundary conditions. This solution is considered further in Appendix A.

In large, homogeneous, source-free systems, the neutron flux is determined predominantly by the value of the dominant eigenvalue κ_1 and so it is useful to compare the value of κ_1, that results from use of a given angular quadrature, with the exact value κ_e. The eigenvalue κ_e can be obtained either by solving Equation (1) or by letting $N \to \infty$ in Equation (6) ; it satisfies the equation

$$\frac{\tanh^{-1}\kappa_e}{\kappa_e} = \frac{1}{c} \quad . \tag{10}$$

A closed expression cannot be obtained for κ_1 unless $N \leq 8$. However, expressions have been obtained for κ_1 as a function of c, $\{\mu_m\}$ and $\{\omega_m\}$ for the limiting cases where $|1-c| << 1$, $c >> 1$ or $c << 1$. A comparison is made with the corresponding expressions for κ_e as a function of c.

2.1 κ_1 when $|1-c| << 1$

An expansion of the form

$$\kappa_1^2 = \sum_{j=1}^{\infty} a_j^1 (1-c)^j \tag{11}$$

is tried. Direct substitution into Equation (6) is difficult. A better approach is to expand $f(\kappa^2)$ of Equation (7) in powers of κ_1^2, to obtain

$$f(\kappa_1^2) = \sum_{h=0}^{\infty} \left[\sum_{m=1}^{N/2} \omega_m \mu_m^{2h} \right] \kappa_1^{2h} \quad , \tag{12}$$

which is valid as long as $|\mu_1 \kappa_1| < 1$. Also,

$$\frac{\tanh^{-1}\kappa_e}{\kappa_e} = \sum_{h=0}^{\infty} \frac{\kappa_e^{2h}}{2h+1} \quad . \tag{13}$$

The coefficients of κ_1^{2h} and κ_e^{2h} agree if

$$\sum_{m=1}^{N/2} \omega_m \mu_m^{2h} = \frac{1}{2h+1} \quad , \tag{14}$$

that is, if the angular quadrature correctly evaluates the moment

$$M_{2h} = \int_0^1 \mu^{2h} d\mu \quad . \tag{15}$$

Since

$$f(\kappa_1^2) = \frac{1}{c} = \frac{\tanh^{-1}\kappa_e}{\kappa_e} \quad , \tag{16}$$

it can be shown by substituting

$$\kappa_1^2 = \sum_{j=1}^{\infty} a_j^1 (1-c)^j$$

and

$$\kappa_e^2 = \sum_{j=1}^{\infty} a_j (1-c)^j$$

in Equation (16), that

$$a_j^1 = a_j \quad (j = 1,2,\ldots J)$$

if the angular quadrature correctly evaluates all moments M_{2h} for $0 \leq h \leq J$.

Hence, the dominant eigenvalue given by a symmetric quadrature which correctly evaluates the moments M_{2h} for $0 \leq h \leq J$, is correct to $0((1-c)^J)$. That is,

$$\kappa_1^2 = \kappa_e^2 + 0\left((1-c)^{J+1}\right) . \tag{17}$$

The following expansion for κ_e has been evaluated by Case, de Hoffman & Placzek (1953):

$$\kappa_e^2 = 3(1-c)\left[1 - 0.8(1-c) + 0.0229(1-c)^2 + 0.0229(1-c)^3 + 0.0224(1-c)^4 + \right.$$
$$\left. + 0.0215(1-c)^5 + \ldots\right] . \tag{18}$$

The result given in Equation (17) also holds when $c > 1$ as long as $|B_1 \mu_1| < 1$ and $|B_e| < 1$.

2.2 B_1 when $c >> 1$

This case is only of academic interest, since large c implies a small system in which all eigenfunctions are important.

Assuming $|\mu_{min} B_1| > 1$, expand

$$f(-B_1^2) = \sum_{m=1}^{N/2} \frac{\omega_m}{1 + \mu_m^2 B_1^2}$$

in powers of B_1^{-2} to obtain the relationship

$$f(-B_1^2) = \sum_{n=1}^{\infty} (-1)^{n+1} b_n B_1^{-2n} , \tag{19}$$

where

$$b_n = \sum_{m=1}^{N/2} \frac{\omega_m}{\mu_m^{2n}} . \tag{20}$$

Expanding B_1^2 in powers of c^{-1}, substituting into Equation (19), equating $f(-B_1^2)$ to $1/c$, and collecting powers of c leads to the relation

$$B_1^2 = b_1 c\left[1 - \frac{b_2}{b_1^2}\left(\frac{1}{c}\right) - \left(\frac{b_2^2}{b_1^4} - \frac{b_3}{b_1^3}\right)\left(\frac{1}{c}\right)^2 - \ldots\right] . \tag{21}$$

This is to be compared with the solution of

$$\frac{\tan^{-1} B_e}{B_e} = \frac{1}{c} ,$$

which is (Case, de Hoffman & Placzek 1953)

$$B_e^2 = \frac{\pi^2 c^2}{4}\left[1 - \frac{8}{\pi^2}\left(\frac{1}{c}\right) - \frac{16}{\pi^4}\left(\frac{1}{c}\right)^2 - \ldots\right] \tag{22}$$

2.3 κ_1 when $c << 1$

For small c, it is apparent from Figure 1 that $\kappa_m^2 \approx 1/\mu_m^2$. A series solution for the dominant eigenvalue κ_1 can be obtained by expanding κ_1^2 in powers of c, substituting in Equation (6), collecting powers of c and equating their coefficients to zero. This leads to

$$\kappa_1^2 = \frac{1}{\mu_1^2}\left[1 - \omega_1 c - \left(\omega_1 \sum_{m=2}^{N/2} \frac{\omega_m \mu_1^2}{\mu_1^2 - \mu_m^2}\right) c^2 - \ldots\right] . \qquad (23)$$

Case, de Hoffman & Placzek (1953) give the following result for κ_e^2:

$$\kappa_e^2 = 1 - 4e^{-2/c}\left[1 + \frac{4 - 2c}{c} e^{-2/c} + \ldots\right] . \qquad (24)$$

The coefficients of c and c^2 in Equation (23) are $0(1/N^2)$ for standard quadrature schemes, so they rapidly decrease for increasing N.

It is apparent from Equations (23) and (24) that the correct evaluation of κ_1 for small c requires μ_1 close to 1.

3. SPATIAL DISCRETISATION – THE DIAMOND DIFFERENCE APPROXIMATION

Replacing the differential coefficient $d\psi_m(x)/dx$ in Equation (4) by the finite difference approximation $(\psi_{m,r+1} - \psi_{m,r})/\Delta$ results in a set of N coupled difference equations:

$$\mu_m [\psi_{m,r+1} - \psi_{m,r}] + \Delta \psi_{m,r+\frac{1}{2}} = \frac{c\Delta}{2} \phi_{r+\frac{1}{2}} , \quad m = 1,2,\ldots,N, \qquad (25)$$

where

Δ is the mesh spacing,

$\psi_{m,r} = \psi_m(r\Delta)$, and

$\psi_{m,r+\frac{1}{2}}$ is some value of $\psi_m(x)$ in the interval $r\Delta$ to $(r + 1)\Delta$.

In the diamond difference method, the approximation

$$\psi_{m,r+\frac{1}{2}} = \frac{1}{2}[\psi_{m,r} + \psi_{m,r+1}] \qquad (26)$$

is used. This leads to the equations

$$\mu_m [\psi_{m,r+1} - \psi_{m,r}] + \frac{\Delta}{2}[\psi_{m,r+1} + \psi_{m,r}] = \frac{c\Delta}{4}[\phi_{r+1} + \phi_r] ,$$

$$m = 1,2,\ldots,N . \qquad (27)$$

These N coupled difference equations may be solved in the following fashion. Substitute $\psi_{m,r+1} = \alpha \psi_{m,r} (m = 1,2,\ldots,N)$ in Equation (27), multiply both sides by $\omega_m / [\mu_m(\alpha - 1) + \frac{\Delta}{2}(\alpha + 1)]$, sum for m = 1 to N and use Equation (3) to obtain the relationship

$$\sum_{m=1}^{N/2} \frac{\omega_m}{1 - \mu_m^2 \left[\frac{2}{\Delta} \cdot \frac{\alpha - 1}{\alpha + 1}\right]^2} = \frac{1}{c} . \qquad (28)$$

Note the similarity between Equations (6) and (28) with κ^2 in the former being replaced by $\left[\frac{2}{\Delta} \cdot \frac{\alpha - 1}{\alpha + 1}\right]^2$ in the latter. If α_m is a solution of Equation (28), then so is $1/\alpha_m$, and there are N/2 independent roots of Equation (28). These have the values

$$\alpha_m = \frac{1 + \kappa_m \Delta/2}{1 - \kappa_m \Delta/2} , \quad m = 1,2,\ldots,N/2 , \qquad (29)$$

where κ_m are the roots of Equation (6). It is apparent that α_m is positive as long as $|\kappa_m \Delta/2| < 1$.

The general solution to Equation (27) has the form

$$\psi_{m,r} = \sum_{i=1}^{N/2} \left[\zeta^c_{m,i} \left(\frac{\alpha_i^r + \alpha_i^{-r}}{2} \right) + \zeta^s_{m,i} \left(\frac{\alpha_i^r - \alpha_i^{-r}}{2} \right) \right] , \quad m = 1,2,\ldots,N \tag{30}$$

where the terms $\zeta^{c,s}_{m,i}$ are constants determined by Equation (27) and by the boundary conditions. For α_m positive, write

$$\alpha_m = e^{\kappa^d_m \Delta} . \tag{31}$$

Then, as long as $|\kappa_{N/2} \Delta/2| < 1$, the general solution to Equation (27) can be written as follows:

$$\text{(i)} \quad \psi_m(r\Delta) = \sum_{i=1}^{N/2} F^r_{m,i} , \quad 0 \leqslant c < 1 ;$$

$$\text{(ii)} \quad \psi_m(r\Delta) = \zeta^c_{m,1} + \zeta^s_{m,1} r\Delta + \sum_{i=2}^{N/2} F^r_{m,i} , \quad c = 1 ;$$

$$\text{(iii)} \quad \psi_m(r\Delta) = \zeta^c_{m,i} \cos(B^d_1 r\Delta) + \zeta^s_{m,i} \sin(B^d_1 r\Delta) + \sum_{i=2}^{N/2} F^r_{m,i} , \quad c > 1 ; \tag{32}$$

where $F^r_{m,i} = \zeta^c_{m,i} \cosh(\kappa^d_i r\Delta) + \zeta^s_{m,i} \sinh(\kappa^d_i r\Delta)$. Note the similarity between Equations (9) and (32), with x and κ_i in the former being replaced by $r\Delta$ and κ^d_i in the latter. Further details of this solution are given in Appendix A.

Equations (29) and (31) give

$$\begin{aligned} \kappa^d_m &= \ell n \left(\frac{1 + \kappa_m \Delta/2}{1 - \kappa_m \Delta/2} \right) / \Delta , \quad |\kappa_m \Delta/2| < 1 \\ &= \tanh^{-1}(\kappa_m \Delta/2)/(\Delta/2) \\ &= \kappa_m \left[1 + \frac{(\kappa_m \Delta)^2}{12} + \frac{(\kappa_m \Delta)^4}{80} + \ldots \right] . \end{aligned} \tag{33}$$

Thus, for the diamond difference method, the eigenvalue κ^d_m can be expressed in terms of the eigenvalue κ_m, resulting from the angular segmentation of the transport equation, as long as $\left| \frac{\kappa_m \Delta}{2} \right| < 1$. From Equation (33), it is apparent that $\kappa^d_m > \kappa_m$ except for $c > 1$, when the relationship for the dominant eigenvalue becomes

$$\begin{aligned} B^d_1 &= \tan^{-1}(B_1 \Delta/2)/(\Delta/2) \\ &= B_1 \left[1 - \frac{(B_1 \Delta)^2}{12} + \frac{(B_1 \Delta)^4}{80} \ldots \right] , \quad \left| \frac{B_1 \Delta}{2} \right| < 1 . \end{aligned} \tag{34}$$

The error in κ^d_m relative to κ_m is second order in Δ and rapidly tends to zero as $\kappa_m \Delta$ becomes small. A value $\kappa_m \Delta = 1.0$ gives $\kappa^d_m = 1.1\ \kappa_m$ while $\kappa_m \Delta = 0.3$ gives $\kappa^d_m = 1.01\ \kappa_m$.

4. SPATIAL DISCRETISATION – THE STEP FUNCTION APPROXIMATION

The step function method uses the approximation

$$\psi_{m,r+\frac{1}{2}} = \psi_{m,r+1} \quad , \quad m = 1,2,\ldots,N/2$$
$$= \psi_{m,r} \quad , \quad m = N/2+1,\ldots,N \qquad (35)$$

in Equation (25). This results in the equations

$$\mu_m\left[\psi_{m,r+1} - \psi_{m,r}\right] + \Delta\psi_{m,r+1} = \frac{c\Delta}{2}\left[\bar{\phi}^+_{r+1} + \bar{\phi}^-_r\right] \qquad m = 1,2,\ldots,N/2,$$

$$\mu_m\left[\psi_{m,r+1} - \psi_{m,r}\right] + \Delta\psi_{m,r} = \frac{c\Delta}{2}\left[\bar{\phi}^+_{r+1} + \bar{\phi}^-_r\right] \qquad m = N/2+1,\ldots,N, \qquad (36)$$

where

$$\bar{\phi}^+_{r+1} = \sum_{m=1}^{N/2} \omega_m \psi_{m,r+1} \quad \text{and} \quad \bar{\phi}^-_r = \sum_{m=N/2+1}^{N} \omega_m \psi_{m,r} \ .$$

Substituting $\psi_{m,r+1} = \alpha\psi_{m,r}$ and proceeding as in Section 3, it is found that α satisfies the the equation

$$\sum_{m=1}^{N/2} \omega_m\left[1 - \frac{\mu_m^2(\alpha-1)^2 + \mu_m(\alpha-1)^2\Delta/2}{\alpha\Delta^2 - \mu_m(\alpha-1)^2\Delta/2}\right]^{-1} = \frac{1}{c} \ . \qquad (37)$$

If α_m is a root of this equation, then so is $1/\alpha_m$; thus there are N/2 independent roots α_m ($m = 1,2,\ldots,N/2$). The evaluation of α_m is simplified by substituting

$$\alpha = \frac{1 + \beta\Delta/2}{1 - \beta\Delta/2} \qquad (38)$$

in Equation (37) which then becomes

$$\sum_{m=1}^{N/2} \omega_m\left[1 - \frac{\mu_m^2\beta^2 + \mu_m\beta^2\Delta/2}{1-\mu_m\beta^2\Delta/2-\beta^2\Delta^2/4}\right]^{-1} = \frac{1}{c} \ . \qquad (39)$$

Consider the function

$$g(\beta^2) = \sum_{m=1}^{N/2} \omega_m\left[1 - \frac{\mu_m^2\beta^2 + \mu_m\beta^2\Delta/2}{1-\mu_m\beta^2\Delta/2-\beta^2\Delta^2/4}\right]^{-1} \ , \qquad (40)$$

which is shown in Figure 2. It has poles at $\beta^2_{p,m} = 1/(\mu_m + \Delta/2)^2$ for $m = 1,2,\ldots,N/2$, and it has limiting values $\lim_{\beta^2 \to \pm\infty} g(\beta^2) = \sum_{m=1}^{N/2} \omega_m/(1 + 2\mu_m/\Delta)$. From Figure 2, it is apparent that there are N/2 values of β_m^2 which satisfy Equation (39) and that $|\beta_m\Delta/2| < 1$ for all real β_m with the exception of the trivial case $c > 1/\sum_{m=1}^{N/2} \omega_m/(1+2\mu_m/\Delta)$, when the mesh size is of the order of, or larger than, the critical size of the medium. Thus, from Equation (38), α_m is positive and it is possible to write

$$\alpha_m = \frac{1 + \beta_m\Delta/2}{1 - \beta_m\Delta/2} = e^{\kappa_m^s\Delta} \ . \qquad (41)$$

The general solution to Equation (36) can now be written in the form given in Equation (32) with

κ_i^s replacing κ_i^d. This general solution is discussed more fully in Appendix A. Although it is not possible to obtain a general expression for κ_m^s in terms of the angular segmentation eigenvalues κ_m, relationships have been derived for the limiting cases of $\Delta \to 0$ and $\Delta \to \infty$.

4.1 Small Spatial Mesh

In this case, an expression for κ_m^s in powers of Δ is most easily achieved by using the expressions

$$\frac{dg(\beta^2)}{d\Delta}\bigg|_{\Delta=0} = 0 \qquad \text{and} \qquad \frac{d^2 g(\beta^2)}{d\Delta^2}\bigg|_{\Delta=0} = 0$$

to obtain expressions for

$$\frac{d\beta^2}{d\Delta}\bigg|_{\Delta=0} \qquad \text{and} \qquad \frac{d^2\beta^2}{d\Delta^2}\bigg|_{\Delta=0} .$$

This gives the first few coefficients in a series expansion of β_m^2 in powers of Δ, and the appropriate expansion for κ_m^s can then be obtained from Equation (41).

After some algebra, the result is

$$\kappa_m^s = \kappa_m [1 - d_m \Delta + e_m \Delta^2 + 0(\Delta^3)] \qquad m = 1,2,\ldots,N/2, \qquad (42)$$

where

$$d_m = \frac{1}{4} \sum_{n=1}^{N/2} \frac{\omega_n \mu_n (1 + \mu_n^2 \kappa_m^2)}{(1-\mu_n^2 \kappa_m^2)^2} \Bigg/ \sum_{n=1}^{N/2} \frac{\omega_n \mu_n^2}{(1-\mu_n^2 \kappa_m^2)^2} . \qquad (43)$$

The expression for e_m is more complicated and is not given here. For large N and $c \simeq 1$, $e_1 \simeq 0.2$. The error in κ_m^s, relative to κ_m, is first order in Δ. The term d_m is positive except for large c, when d_1 becomes negative. Thus, use of the step function approximation leads to eigenvalues κ_m^s which are smaller than the corresponding eigenvalues κ_m. For the dominant eigenvalue κ_1^s, the following expression can be obtained for d_1 in the limit of large N:

$$\lim_{N\to\infty} d_1 = \left[\frac{\kappa_1^2}{1-\kappa_1^2} + \frac{1}{2} \ell_n (1-\kappa_1^2)\right] \Bigg/ \left[\frac{2}{1-\kappa_1^2} - \frac{1}{\kappa_1} \ell_n \frac{1+\kappa_1}{1-\kappa_1}\right] . \qquad (44)$$

For $c > 1$, the expressions for d_1 are obtained from Equations (43) and (44) by replacing κ_1 by iB_1. Values of d_1 as a function of N and c are given in Table 1. Typical values of d_1 are about 0.4 and a mesh size as small as $\Delta = 0.1$ will lead to a 4 per cent error in κ_1^s relative to κ_1. It is interesting to note that for small Δ and $c \simeq 1$, $\kappa_1^d = \kappa_1 (1 + 0(1-c) \cdot 0(\Delta^2))$ whereas $\kappa_1^s = \kappa_1 (1 + 0(1) \cdot 0(\Delta))$.

The radius of convergence of the expansion in Equation (42) has not been found except in the case of $c = 0$, when the expression converges as long as $|\Delta/(2\mu_m)| < 1$. This is probably a conservative criterion for convergence when $0 < c \leq 1$.

4.2 Large Spatial Mesh

The expression in Equation (42) is only accurate for $|d_m \Delta| \lesssim 0.1$, so an alternative expression is sought for large Δ. The case $c > 1$ is not treated since negative flux values are obtained for multiplying media for large Δ.

TABLE 1

VALUES OF d_1 AND κ_1 USING GAUSS–LEGENDRE QUADRATURE

	d_1			$\kappa_1(B_1)$		
c \ N	2	4	∞	2	4	∞
>>1	–0.433c	–0.581c	$-0.5c\,\ell_n\,c$	$1.732c^{½}$	$2.472c^{½}$	$0.5\,\pi c$
2.0	0.000	0.027	–0.125	1.732	2.164	2.331
1.5	0.217	0.237	0.159	1.225	1.443	1.451
1.1	0.390	0.364	0.339	0.548	0.569	0.569
1.0	0.433	0.391	0.375	0.000	0.000	0.000
0.9	0.477	0.417	0.407	0.548	0.526	0.525
0.5	0.649	0.509	0.488	1.225	0.989	0.958
0.0	0.866	0.581	0.500	1.732	1.161	1.000

Note: For c = 1 and N = ∞, $e_1 = 27/128 = 0.211$

Using the definition

$$\beta = \frac{1}{\gamma + \Delta/2} \quad , \tag{45}$$

the following useful expression for κ_m^s can be deduced:

$$\kappa_m^s = \frac{1}{\Delta}\ \ell_n\left(\frac{\Delta}{\gamma_m} + 1\right) , \tag{46}$$

where γ_m are roots of the equation

$$\sum_{m=1}^{N/2} \frac{\omega_m[\gamma^2 + (\gamma - \mu_m/2)\Delta]}{(\gamma - \mu_m)(\gamma + \mu_m + \Delta)} = \frac{1}{c} \quad , \tag{47}$$

with the following limits:

$$\mu_1 \leqslant \gamma_1 \leqslant \infty \qquad \text{and} \qquad \mu_m \leqslant \gamma_m < \mu_{m-1} , \quad m = 2,3,\ldots,N/2 .$$

The γ_m are functions of both c and Δ. The power series expansion

$$\gamma = \gamma^0 + \gamma^1/\Delta + 0\,(1/\Delta^2) \tag{48}$$

is substituted into Equation (47). Only the first term in Equation (48) is retained owing to the increasingly complex analysis needed for higher terms. This leads to the equation

$$\sum_{m=1}^{N/2} \frac{\omega_m(\gamma^0 - \mu_m/2)}{\gamma^0 - \mu_m} = \frac{1}{c} \tag{49}$$

for the values γ_m^0 . A closed expression cannot be obtained for γ_m^0 as a function of c , so an expansion of γ^0 in powers of (1–c) and c is used with the following results.

For $|1-c| << 1$, the dominant eigenvalue is given by

$$\kappa_1^s = \frac{1}{\Delta} \ell_n \left(\frac{\Delta}{\gamma_1^0} + 0(1) \right) \tag{50}$$

with

$$\gamma_1^0 = \frac{\sum_{m=1}^{N/2} \omega_m \mu_m}{2(1-c)} + \frac{\sum_{m=1}^{N/2} \omega_m \mu_m^2 - \frac{1}{2}\left[\sum_{m=1}^{N/2} \omega_m \mu_m\right]^2}{\sum_{m=1}^{N/2} \omega_m \mu_m} + 0(1-c)$$

$$= \frac{1}{4(1-c)} + \frac{5}{12} + 0(1-c) \quad , \quad \text{for N large} \quad . \tag{51}$$

This result is accurate when $0 \leqslant (1-c) << 1$ and $(1-c)\,\Delta >> 1$.

For $c << 1$, the eigenvalues are given by

$$\kappa_m^s = \frac{1}{\Delta} \ell_n \left(\frac{\Delta}{\gamma_m^0} + 0(1) \right) \tag{52}$$

with

$$\gamma_m^0 = \mu_m + 0.5\, \omega_m \mu_m\, c + 0(c^2) \quad , \quad m = 1,2,\ldots,N/2 \tag{53}$$

$$= \mu_m \quad , \quad \text{for N large} \quad .$$

5. ANISOTROPIC SCATTERING

The preceding analysis is now expanded to include the effects of anisotropic scattering. Only the more interesting aspects are considered because of the complexity of the eigenvalue equations that are obtained.

The extension of Equation (1) to include anisotropic scattering up to order L gives

$$\mu \frac{\partial \psi(x,\mu)}{\partial x} + \psi(x,\mu) = \frac{c}{2} \sum_{\ell=0}^{L} (2\ell+1)\, b_\ell\, \phi_\ell(x)\, P_\ell(\mu) \quad , \tag{54}$$

where

$$\phi_\ell(x) = \int_{-1}^{1} \psi(x,\mu) P_\ell(\mu)\, d\mu \tag{55}$$

and the scattering function

$$f(\underset{\sim}{\Omega}' \cdot \underset{\sim}{\Omega}) = f(\mu_0) = \frac{1}{4\pi} \sum_{\ell=0}^{L} (2\ell+1)\, b_\ell P_\ell(\mu_0) \, . \tag{56}$$

The terms b_ℓ are the Legendre components of the scattering function, with $b_0 = 1$.

An equation for the eigenvalues of Equation (54) is now derived. Assume a separable flux of the form

$$\psi(x,\mu) = e^{\kappa x}\, \xi(\kappa,\mu) \tag{57}$$

with

$$\xi(\kappa,\mu) = \frac{1}{2} \sum_{\ell=0}^{\infty} (2\ell + 1)\, \zeta_\ell(\kappa)\, P_\ell(\mu) \quad . \tag{58}$$

Substitute Equation (57) into Equation (54), multiply by $P_n(\mu)$ and integrate over μ to obtain the equations

$$(n+1)\, \zeta_{n+1}(\kappa) + (1-cb_n)(2n+1)\, \zeta_n(\kappa)/\kappa + n\, \zeta_{n-1}(\kappa) = 0 , \quad n \geq 0 . \tag{59}$$

These equations can be solved for $\zeta_n(\kappa)$ in terms of $\zeta_0(\kappa)$, and $\zeta_0(\kappa)$ can be normalised to unity. Another equation for $\zeta_n(\kappa)$ is obtained by substituting Equation (57) into Equation (54), multiplying by $P_n(\mu)/(1+\mu\kappa)$ and integrating over μ. This gives

$$\zeta_n(\kappa) = \frac{c}{2} \sum_{\ell=0}^{L} (2\ell + 1)\, b_\ell\, \zeta_\ell(\kappa) \int_{-1}^{1} \frac{P_n(\mu)\, P_\ell(\mu)}{1+\mu\kappa}\, d\mu \quad . \tag{60}$$

Substitution of $n = 0$ in Equation (60) gives the eigenvalue equation

$$1 = \frac{c}{2} \sum_{\ell=0}^{L} (2\ell + 1)\, b_\ell\, \zeta_\ell(\kappa) \int_{-1}^{1} \frac{P_\ell(\mu)}{1+\mu\kappa}\, d\mu \quad . \tag{61}$$

Mika (1961) has found that there are, at most, 2(L+1) discrete roots of Equation (61) of the form $\pm\kappa$, and for $c = 1$ there is a double root, $\kappa = 0$. In Appendix B it is shown that as long as $|1-c| << 1$ and $b_\ell \neq 1$ for $\ell > 0$, the smallest eigenvalue, κ_e, can be expressed in the form

$$\kappa_e^2 = f_1(b_1)\,(1-c) + f_2(b_1,b_2)\,(1-c)^2 + \ldots + f_L(b_1,\ldots,b_L)\,(1-c)^L + \\ + f_{L+1}(b_1,\ldots,b_L)\,(1-c)^{L+1} + \ldots \tag{62}$$

and

$$\zeta_\ell(\kappa_e) = 0\left((1-c)^{\ell/2}\right) \quad . \tag{63}$$

From Equation (62), it is apparent that if the expansion of the scattering function has been truncated at order L, then κ_e^2 is accurate to $0\left((1-c)^L\right)$.

5.1 Angular Segmentation

The relationship between the eigenvalue κ_e and the corresponding eigenvalue κ_1, obtained from the S_N form of Equation (54), is now determined under the condition that $|1-c| << 1$. After angular segmentation, Equation (54) becomes

$$\mu_m \frac{d\psi_m(x)}{dx} + \psi_m(x) = \frac{c}{2} \sum_{\ell=0}^{L} (2\ell + 1)\, b_\ell\, \bar{\phi}_\ell(x)\, P_\ell(\mu_m) \quad , \tag{64}$$

where

$$\bar{\phi}_\ell(x) = \sum_{m=1}^{N} \omega_m\, \psi_m(x)\, P_\ell(\mu_m) \quad . \tag{65}$$

Assume a separable flux of the form

$$\psi_m(x) = e^{\kappa x}\, \xi_m(\kappa) \tag{66}$$

and define

$$\bar{\zeta}_\ell(\kappa) = \sum_{m=1}^{N} \omega_m\, \xi_m(\kappa)\, P_\ell(\mu_m) \quad . \tag{67}$$

Substitute Equation (66) into Equation (64), multiply by $\omega_m P_n(\mu_m)/(1+\mu_m\kappa)$ and sum over m to obtain the equation

$$\bar{\zeta}_n(\kappa) = \frac{c}{2}\sum_{\ell=0}^{L}(2\ell+1)b_\ell\,\bar{\zeta}_\ell(\kappa)\sum_{m=1}^{N}\frac{\omega_m P_n(\mu_m)P_\ell(\mu_m)}{1+\mu_m\kappa} \quad . \tag{68}$$

Taking n = 0 and defining $\bar{\zeta}_0(\kappa) = 1$, Equation (68) becomes

$$1 = \frac{c}{2}\sum_{\ell=0}^{L}(2\ell+1)b_\ell\,\bar{\zeta}_\ell(\kappa)\sum_{m=1}^{N}\frac{\omega_m P_\ell(\mu_m)}{1+\mu_m\kappa} \quad . \tag{69}$$

There are N eigenvalues of the form $\pm\kappa_m (m = 1,2,\ldots,N/2)$ which satisfy Equation (69). The smallest one, κ_1, tends to zero as $c \to 1$.

Comparisons of Equation (68) with Equation (60) and Equation (69) with Equation (61) show, after some algebra, that

$$\kappa_1^2 = \kappa_e^2 + 0\left((1-c)^{J+1}\right) \tag{70}$$

and

$$\bar{\zeta}_\ell(\kappa_1) = \zeta_\ell(\kappa_e)\left[1 + 0\left((1-c)^{J+1-\ell}\right)\right] \quad , \tag{71}$$

when the quadrature evaluates the moments

$$M_{2h} = \int_0^1 \mu^{2h}\,d\mu$$

correctly for $0 \leqslant h \leqslant J$.

It is apparent from Equations (62) and (70) that, at least for $|1-c| << 1$, a value of $J \geqslant L$ is necessary if the error in κ_1 is to be of the same order as any error in κ_e arising from the truncation of the anisotropic scattering at order L.

5.2 Spatial Discretisation – the Diamond Difference Approximation

An analysis similar to that carried out in Section 3 can be applied to Equation (64) using the diamond difference approximation. This leads to the same results as obtained in Section 3, namely, that there are N eigenvalues of the form $\pm\kappa_m^d$, which are related to the eigenvalues of Equation (69) by

$$\kappa_m^d = \tanh^{-1}(\kappa_m\Delta/2)/(\Delta/2) \tag{72}$$

if $|\kappa_m\Delta/2| < 1$.

5.3 Spatial Discretisation – the Step Function Approximation

An analysis similar to that carried out in Section 4 has been applied to Equation (64). This leads to an expression for the eigenvalues κ_m^s which involves a determinant of order L + 1. Substitution of an expansion of the form

$$\kappa_m^s = \kappa_m[1 - d_m\Delta + 0(\Delta^2)] \tag{73}$$

into this expression results in an equation for d_m which is quite complex. A value of d_m has been obtained for the special case of L = 1, but even in this case the equation is not simple and so is not given here. However, it can be shown that for $c \simeq 1$,

$$d_1 = \frac{3}{8}(1-b_1) + 0(1-c) \quad . \tag{74}$$

When inserted in Equation (73) this gives, for $c \simeq 1$, the same value for κ_1^s as would be obtained by using the isotropic scattering value of d_1 and measuring Δ in transport mean free paths. Also, when $c << 1$, the transport mean free path is the same as the total mean free path and the values of d_1 for isotropic and anisotropic scattering are identical. Thus it appears that a feasible method for the evaluation of the correction term $d_1\Delta$ in Equation (73) is to evaluate d_1 from Equation (43) and measure Δ in transport mean free path units. It is conjectured that this approach can also be used for the evaluation of $d_1\Delta$ when higher order anisotropic scattering is included.

To test this conjecture, the transport theory code ANISN (Engle 1967) was used to evaluate the neutron flux in a 120 cm water slab with a source on the left hand boundary. One–group cross sections corresponding to an energy range of 10 MeV $\geqslant$ E $\geqslant$ 1 MeV were used, with scattering included up to order P3. A single exponential of the form $\exp(-\kappa x)$ was fitted to the flux between x = 20 cm and x = 80 cm, and κ was evaluated for a fine spatial mesh and for a mesh of 2 cm. For the fine mesh, $\kappa = 0.206$ cm^{-1} while the 2 cm mesh gave $\kappa = 0.176$ cm^{-1}. The value of κ predicted by Equation (43) for the 2 cm mesh was 0.166 cm^{-1} for Δ measured in total mean free paths, and 0.175 cm^{-1} for Δ measured in transport mean free paths.

These results support the above conjecture that, when the step function approximation is used, Equation (43) gives a good estimate of the variation with spatial mesh of the dominant eigenvalue as long as the mesh is measured in transport mean free paths.

6. MULTIGROUP AND MULTIDIMENSIONAL PROBLEMS

Because of the complexity of the solution, a direct extension of the analysis presented in this report is not feasible for multigroup and multidimensional problems. However, in many classes of problems the flux has certain similarities to a one–group, slab geometry flux and so the results derived for the latter may be adequate. In particular, the radiation shield of a reactor generally has a large radius of curvature, and often consists of a thick homogeneous material in which the flux attenuation is governed by the behaviour of the high energy neutrons (E > 1 MeV). In this case, the neutron spectrum varies only slowly with distance into the shield, and the flux behaviour resembles that of a monoenergetic flux in a slab.

Before considering an explicit example to illustrate this situation, an analysis is made of the dependence of a multigroup flux on angular and spatial mesh. All aspects of the multigroup transport equation which are of interest here can be examined by considering a one–group equation, with a specified source which represents the in–scatter from other groups. A large homogeneous region is assumed and the source is taken to have a spatial dependence of the form

$$S(x) = S_o \exp(-\kappa_{so} x) \quad . \tag{75}$$

Two possibilities arise, depending whether the dominant eigenvalue, κ, of the group under consideration is smaller or larger than κ_{so}.

(1) $\kappa < \kappa_{so}$

In this case the source dies away faster than the flux with penetration into the region. Thence the flux behaves as a one–group, source–free flux after a certain distance into the medium.

(2) $\kappa > \kappa_{so}$

In this case the flux has a spatial variation similar to the source term,

$$\phi(x) = \phi_o \exp(-\kappa_{so} x) \quad . \tag{76}$$

However, the amplitude of the flux, ϕ_o, is dependent on the angular quadrature and the mesh size. The dependence of ϕ_o on the angular quadrature and spatial mesh can be analysed using tech–

niques similar to those in Sections 2 to 5. The results obtained are now outlined. In the following, the further approximation is made that S_o and κ_{so} are constant and independent of the meshes used.

(2a) If ϕ_o^a is the value obtained using an infinitesimal spatial mesh and an angular quadrature which evaluates moments $M_{2h} = \int_0^1 \mu^{2h}\, d\mu$ correctly for $0 \leqslant h \leqslant J$, and ϕ_o is the exact value, then

$$\phi_o^a = \phi_o \left[1 + 0\left(\kappa_{so}^{2(J+1)}\right)\right] \quad . \tag{77}$$

(2b) If ϕ_o^{dd} is the value obtained using the above angular quadrature and the diamond difference approximation, then

$$\phi_o^{dd} = \phi_o^a \left[1 + 0\left((\kappa_{so}\Delta)^2\right)\right] \quad . \tag{78}$$

This result assumes that oscillations do not perturb the flux.

(2c) If ϕ_o^s is the value obtained using the above angular quadrature and the step function approximation, then

$$\phi_o^s = \phi_o^a \left[1 + 0\left(\kappa_{so}\Delta\right)\right] \quad . \tag{79}$$

It can be deduced from the above relations for $\kappa > \kappa_{so}$, that mesh sizes which lead to the accurate evaluation of the source term $S_o \exp(-\kappa_{so}x)$ will also give accurate values for the flux $\phi(x)$, provided that $\phi(x)$ has the spatial dependence $\exp(-\kappa_{so}\, x)$.

As a test of the applicability of the one–group results for a typical multigroup problem encountered in reactor shielding, the transport theory code ANISN (Engle 1967) has been used to evaluate the S8(P3), 29–group neutron flux arising from a fission spectrum source at the left hand boundary of a 120 cm water slab. In this case, the attenuation of the flux is determined predominantly by the behaviour of the fast neutrons with energy greater than 1 MeV. To evaluate the dependence of the fast flux on the spatial mesh used in the solution of the transport equation, the neutron flux in the first 11 groups (E > 1 MeV) was calculated using the diamond difference approximation for mesh widths of 1 cm, 2 cm and 4 cm, and each total flux was fitted by an exponential of the form $\exp(-\kappa x)$ between x = 20 cm and x = 80 cm. The derived values of κ for the 1 cm and 2 cm mesh were 0.1355 and 0.1359 respectively. The difference in these values is 0.0004, which is about 30 per cent less than the difference of 0.0006 predicted by Equation (33). Flux oscillations are evident in the 4 cm mesh case and so an exponential attenuation no longer describes the flux. From this analysis it appears that the accuracy of the diamond difference approximation will not generally be limited by the mesh size dependence of the dominant eigenvalue, but by the flux oscillations arising from negative values of the eigenvalues α_m, defined in Equation (29).

The flux has also been evaluated using the step function approximation with a 1 cm mesh, giving the result κ = 0.1304. A difficulty encountered here is the value of the transport mean free path to be used as the unit of length in Equation (42) for the prediction of the mesh size effect on the eigenvalue. A flux average of the transport mean free path using the flux spectrum at x = 50 cm was tried, but this gives a correction term which was 70 per cent too large. Better results would be obtained if a larger mean free path was used. This indicates that the attenuation rate from x = 20 cm to x = 80 cm is determined mainly by the flux at an energy near the upper part of the 1 to 10 MeV range, as the mean free path becomes larger with increasing energy.

It is felt that the results obtained in this example are adequate in that they show that, when the multigroup flux can be fitted by an exponential over a considerable spatial range, the one–group results can be used to predict the approximate effect of the spatial mesh size upon the results, and hence indicate whether the mesh used in a particular problem is small enough.

7. SUMMARY

The discrete ordinates form of the one–group neutron transport equation has been solved analytically in order to show the dependence of the solution on the angular quadrature and spatial mesh used. The results obtained are predominantly of interest for the case of a large homogeneous system in which the flux can be characterised by a function of the form $\exp(-\kappa x)$, where the dominant eigenvalue κ may be real or imaginary. The dependence of κ on the angular quadrature and on the spatial mesh has been examined.

Assuming an infinitesimal spatial mesh and isotropic scattering, the relationship between the dominant eigenvalue, κ_1, obtained from the S_N equation and the exact value, κ_e, can be expressed by the relationship

$$\kappa_1^2 = \kappa_e^2 + 0\left((1-c)^{J+1}\right) \quad , \tag{80}$$

where $c = \sigma_s/\sigma_t$ and the angular quadrature is symmetric and evaluates the moments $M_{2h} = \int_0^1 \mu^{2h}\, d\mu$ correctly for $0 \leq h \leq J$. This relationship also holds for anisotropic scattering as long as $|1-c| << 1$ and the scattering parameters $b_\ell \neq 1$ for $\ell > 0$. It has been shown that if the Legendre expansion of the anisotropic scattering term is approximated by L terms, then κ_e^2 is accurate to $0\left((1-c)^L\right)$. Therefore, to retain this order of accuracy, it is necessary that the angular quadrature evaluates the moments M_{2h} for $0 \leq h \leq L$.

For problems in which absorption is small and in which the neutron flux is characterised by a function of the form $\exp(-\kappa x)$, Equation (80) indicates that an angular quadrature which evaluates the largest number of moment terms, M_{2h}, will generally be most accurate. This points to the use of Gauss–Legendre quadrature for large systems with slab or spherical geometry. For a problem with high absorption, $c << 1$, the dominant eigenvalue may not play such a large part in the determination of the flux. When it does, a quadrature which has a concentration of terms in the direction of greatest flux decrease may give the greatest accuracy; however, the accuracy of the quadrature used will be very problem–dependent.

The use of a finite spatial mesh for the flux evaluation also has an effect upon the dominant eigenvalue obtained. The diamond difference approximation results in a dominant eigenvalue κ_1^d, related to κ_1 by

$$\kappa_1^d = \tanh^{-1}(\kappa_1\Delta/2)/(\Delta/2)$$
$$= \kappa_1\left[1 + \frac{(\kappa_1\Delta)^2}{12} + \frac{(\kappa_1\Delta)^4}{80} + \ldots\right] \quad , \tag{81}$$

as long as $\kappa_1\Delta/2 < 1$, where Δ is the spatial mesh size. This eigenvalue will determine the flux in a large homogeneous system as long as the larger eigenvalues, κ_n $(n = 2, \ldots, N/2)$, satisfy $\kappa_n\Delta/2 < 1$. If this condition is not satisfied, spurious flux oscillations and/or negative flux values may occur and the flux will not be given by a term of the form $\exp(-\kappa x)$. Equation (81) shows that for $c < 1$, κ_1^d is greater than κ_1 and so the diamond difference approximation results in a flux which falls off faster with increasing x than does the flux evaluated using an infinitesimal mesh. However, the eigenvalue correction term, $(\kappa_1\Delta)^2/12$, is generally small and the effective limitation on the mesh size used in the diamond difference approximation is caused by the appearance of flux oscillations due to a too large mesh, rather than by the error in the dominant eigenvalue.

The step function approximation for finite spatial mesh results in a dominant eigenvalue (κ_1^s) which, for isotropic scattering and small Δ, is related to κ_1 by

$$\kappa_1^s = \kappa_1\left[1 - d_1\Delta + e_1\Delta^2 + 0(\Delta^3)\right] \quad , \tag{82}$$

where $d_1 \simeq 0.4$, $e_1 \simeq 0.2$ and Δ is the spatial mesh measured in mean free path units. In the presence of anisotropic scattering, Equation (82) holds quite well when Δ is expressed in transport mean free path units. The eigenvalue κ_1^s is less than κ_1, and so the step function approximation overestimates the value of an exponentially decreasing flux. Also, the eigenvalue correction term $-d_1\Delta$ is small only when $\Delta << 1$, and so an accurate calculation of a large homogeneous system requires the use of a spatial mesh which is a small fraction of a mean free path.

For a problem representative of a class of deep penetration shielding problems, the equations derived for the one–group case have been used to predict the dependence of the multigroup flux on the spatial mesh used, and the prediction has been compared with the actual dependence. The results show that for problems in which the flux can be approximately represented by a function of the form $\exp(-\kappa x)$, the one–group equations can be used to estimate the variation of the eigenvalue κ with spatial mesh size, and so present a method of evaluating whether or not the spatial mesh used is small enough for the desired accuracy.

8. REFERENCES

Case, K.M., Hoffmann, F. de & Placzek, G. (1953) – Introduction to the Theory of Neutron Diffusion. US Government Printing Office, Washington.

Davison, B. (1957) – Neutron Transport Theory. Oxford University Press, London.

Engle, Jr. W.W. (1967) – ANISN, A one dimensional discrete ordinates transport theory code. K–1693.

Mika, J.K. (1961) – Neutron transport with anisotropic scattering. Nucl. Sci. Eng., 11, 415.

APPENDIX A

THE EIGENFUNCTIONS OF THE DISCRETE ORDINATES EQUATIONS

The general solution of the angular segmented transport equation

$$\mu_m \frac{d\psi_m(x)}{dx} + \psi_m(x) = \frac{c\phi}{2} \qquad \text{(A1)}$$

is given in Equation (9). This solution contains N^2 constants, $N(N-1)$ of which can be evaluated by substituting Equation (9) into Equation (A1). This results in the following general solution of Equation (A1):

$$\text{(i)} \quad \psi_m(x) = \sum_{i=1}^{N/2} G_{m,i}(x) \qquad c < 1 \ ;$$

$$\text{(ii)} \quad \psi_m(x) = \zeta_1^+ + \zeta_1^-(x-\mu_m) + \sum_{i=2}^{N/2} G_{m,i}(x) \qquad c = 1 \ ;$$

$$\text{(iii)} \quad \psi_m(x) = \zeta_1^+ \frac{\cos(B_1 x) + \mu_m B_1 \sin(B_1 x)}{1 + \mu_m^2 B_1^2} + \zeta_1^- \frac{\sin(B_1 x) - \mu_m B_1 \cos(B_1 x)}{1 + \mu_m^2 B_1^2} + \sum_{i=2}^{N/2} G_{m,i}(x)$$

$$c > 1 \ ; \qquad \text{(A2)}$$

where

$$G_{m,i}(x) = \frac{\zeta_i^+ e^{\kappa_i x}}{1 + \mu_m \kappa_i} + \frac{\zeta_i^- e^{-\kappa_i x}}{1 - \mu_m \kappa_i} \qquad \text{(A3)}$$

and the terms $\zeta_i^{+,-}$ are constants to be fixed by the boundary conditions.

The diamond difference form of the transport equation,

$$\mu_m[\psi_{m,r+1} - \psi_{m,r}] + \frac{\Delta}{2}[\psi_{m,r+1} + \psi_{m,r}] = \frac{c\Delta}{4}[\bar{\phi}_{r+1} + \bar{\phi}_r] \ , \qquad \text{(A4)}$$

has the general solution given in Equation (30). Substituting Equation (30) into Equation (A4) results in the following expression for the general solution:

$$\psi_m(r\Delta) = \sum_{i=1}^{N/2} \left[\frac{\zeta_i^+ \alpha_i^r}{1 + \mu_m \kappa_i} + \frac{\zeta_i^- \alpha_i^{-r}}{1 - \mu_m \kappa_i} \right] \ , \qquad \text{(A5)}$$

where $\zeta_i^{+,-}$ are constants determined by the boundary conditions. If $|\kappa_{N/2}\,\Delta/2| < 1$, the solution (A5) can be written as:

$$\text{(i)} \quad \psi_m(r\Delta) = \sum_{i=1}^{N/2} G_{m,i}^r \qquad c < 1 \ ;$$

$$\text{(ii)} \quad \psi_m(r\Delta) = \zeta_1^+ + \zeta_1^-(r\Delta - \mu_m) + \sum_{i=2}^{N/2} G_{m,i}^r \qquad c = 1 \ ;$$

$$\text{(iii)} \quad \psi_m(r\Delta) = \zeta_1^+ \frac{\cos(B_1^d r\Delta) + \mu_m B_1 \sin(B_1^d r\Delta)}{1 + \mu_m^2 B_1^2} + \zeta_1^- \frac{\sin(B_1^d r\Delta) - \mu_m B_1 \cos(B_1^d r\Delta)}{1 + \mu_m^2 B_1^2} + \sum_{i=2}^{N/2} G_{m,i}^r$$

$$c > 1 \ ; \qquad \text{(A6)}$$

APPENDIX A (continued)

where

$$G^{r}_{m,i} = \frac{\zeta_i^{+} e^{\kappa_i^d r\Delta}}{1+\mu_m \kappa_i} + \frac{\zeta_i^{-} e^{-\kappa_i^d r\Delta}}{1-\mu_m \kappa_i} \qquad \text{(A7)}$$

and $\zeta_i^{+,-}$ are constants to be fixed by the boundary conditions. Note the similarity between Equations (A6) and (A2), with $\kappa_i^d r\Delta$ replacing $\kappa_i x$ in the exponential, sine and cosine terms.

The step function form of the transport equation,

$$\mu_m [\psi_{m,r+1} - \psi_{m,r}] + \Delta\psi_{m,r+1} = \frac{c\Delta}{2} [\bar{\phi}^{+}_{r+1} + \bar{\phi}^{-}_{r}] \qquad m \leq N/2$$

$$\mu_m [\psi_{m,r+1} - \psi_{m,r}] + \Delta\psi_{m,r} = \frac{c\Delta}{2} [\bar{\phi}^{+}_{r+1} + \bar{\phi}^{-}_{r}] \qquad m > N/2 , \qquad \text{(A8)}$$

has a general solution similar to that given in Equation (30). Substituting Equation (30) into Equation (A8) results in the following expression for the general solution:

$$\psi_m(r\Delta) = \sum_{i=1}^{N/2} \left[\frac{\zeta_i^{+} \alpha_i^{r}}{1+\nu_m\beta_i} + \frac{\zeta_i^{-} \alpha_i^{-r}}{1-\nu_m\beta_i} \right] , \qquad \text{(A9)}$$

where

$$\nu_m = \mu_m + \Delta/2 \qquad m \leq N/2$$

$$= -(|\mu_m| + \Delta/2) \qquad m > N/2 , \qquad \text{(A10)}$$

and β_i has been defined in Equation (38). Putting $\alpha_i = e^{\kappa_i^s \Delta}$ in Equation (A10), the general solution of the step function equations can be written in the form given in Equation (A6), with the replacement of κ_i^d by κ_i^s, κ_i by β_i and μ_m by ν_m.

APPENDIX B

THE DOMINANT EIGENVALUE WITH ANISOTROPIC SCATTERING

It is shown that the dominant eigenvalue, κ_e, has an expansion in powers of (1–c) for $|1-c| << 1$ and $b_\ell \neq 1$, $\ell > 0$.

From Section 5, κ_e satisfies the equations

$$(n+1)\,\zeta_{n+1}(\kappa_e) + (1-cb_n)\,(2n+1)\,\zeta_n(\kappa_e)/\kappa_e + n\,\zeta_{n-1}(\kappa_e) = 0, \quad n \geq 0 \tag{B1}$$

and

$$\zeta_n(\kappa_e) = \frac{c}{2} \sum_{\ell=0}^{L} (2\ell+1) b_\ell\, \zeta_\ell(\kappa_e) \int_{-1}^{1} \frac{P_n(\mu) P_\ell(\mu)}{1+\mu\kappa_e}\, d\mu \quad . \tag{B2}$$

To obtain the expansion for κ_e it is necessary to show that

$$\zeta(\kappa_e) = 0\left((1-c)^{\ell/2}\right) = 0(\kappa_e^\ell) \quad . \tag{B3}$$

First note that Davison (1957) has shown that $\kappa_e \propto (1-c)^{1/2}$ if $b_1 \neq 1$.

Also,

$$\int_{-1}^{1} \frac{P_n(\mu) P_\ell(\mu)}{1+\kappa_e}\, d\mu = 0(\kappa_e^{|n-m|})\,\{1+0(\kappa_e^2)\} \quad . \tag{B4}$$

Substitution of Equation (B4) into Equation (B2) shows that if $\zeta_\ell = 0(\kappa_e^\epsilon)$, then $\zeta_{\ell+1} = 0(\kappa_e^{\epsilon+1})$ for $\ell > L$. Hence, from Equation (B1) it is seen that $\zeta_{\ell-1} = 0(\kappa_e^{\epsilon-1})$. Repeated use of Equation (B1) gives $\zeta_o = 0(\kappa_e^{\epsilon-\ell})$, as long as $b_n \neq 1$ for $n > 0$; but $\zeta_o = 1$ so $\epsilon = \ell$ and Equation (B3) holds.

To obtain the expansion for κ_e consider Equation (B2) with $n = 0$.

This is

$$1 = \frac{c}{2} \sum_{\ell=0}^{L} (2\ell+1) b_\ell\, \zeta_\ell(\kappa_e) \int_{-1}^{1} \frac{P_\ell(\mu)}{1+\mu\kappa_e}\, d\mu \quad . \tag{B5}$$

Substitution of Equations (B3 and (B4) into Equation (B5) shows that

$$1 = c \sum_{\ell=0}^{L} b_\ell 0(\kappa_e^{2\ell}) \quad . \tag{B6}$$

As κ_e^2 is 0(1–c), it is apparent that the series expansion of κ_e in powers of (1–c) has the form

$$\kappa_e^2 = f_1(b_1)(1-c) + f_2(b_1,b_2)(1-c)^2 + \ldots + f_L(b_1,b_2,\ldots,b_L)(1-c)^L + \\ + f_{L+1}(b_1,b_2,\ldots,b_L)(1-c)^{L+1} + \ldots, \tag{B7}$$

for $|1-c| << 1$ and $b_\ell \neq 1$ for $\ell > 0$. Evaluation of the coefficients f_ℓ is arduous, so only the three following values have been obtained:

$$f_1(b_1) = 3(1-b_1) \tag{B8}$$

APPENDIX B (continued

$$f_2(b_1,b_2) = 3b_1 - (12/5)\,(1-b_1)/(1-b_2) \qquad \text{(B9)}$$

$$f_3(b_1,b_2,b_3) = (12/5)\,(1-b_1)/(1-b_2)\,\left[(4/5 + b_2)/(1-b_2) - \right.$$

$$\left. - b_1/(1-b_1) - (27/35)\,(1-b_1)/\left((1-b_2)\,(1-b_3)\right)\right] \qquad \text{(B10)}$$

APPENDIX C

THE EIGENVALUES OF THE FINITE DIFFERENCE DIFFUSION THEORY EQUATION

The one–group, time–independent, source–free neutron diffusion equation in slab geometry can be written as:

$$\nabla^2 \phi(x) - \kappa^2 \phi(x) = 0 \quad . \tag{C1}$$

Taking the usual three point finite difference approximation for the Laplacian, Equation (C1) becomes:

$$\frac{\phi_{n+1} - 2\phi_n + \phi_{n-1}}{\Delta^2} - \kappa^2 \phi_n = 0 \; . \tag{C2}$$

Substituting $\phi_{n+1} = \alpha \phi_n = \alpha^2 \phi_{n-1}$ in Equation (C2) leads to the relationship

$$\alpha^2 - (2 + \kappa^2 \Delta^2)\alpha + 1 = 0 \quad . \tag{C3}$$

The two roots of Equation (C3) are α and $1/\alpha$, where

$$\alpha = 1 + \kappa^2 \Delta^2/2 + \kappa \Delta (1 + \kappa^2 \Delta^2/4)^{1/2} \quad . \tag{C4}$$

Defining the eigenvalue κ' by

$$\alpha = e^{\kappa' \Delta} \tag{C5}$$

gives

$$\begin{aligned} \kappa' &= \frac{1}{\Delta} \tanh^{-1} \left[\frac{\alpha - \alpha^{-1}}{\alpha + \alpha^{-1}} \right] \\ &= \frac{1}{\Delta} \tanh^{-1} \left[\frac{\kappa \Delta (1 + \kappa^2 \Delta^2/4)^{1/2}}{1 + \kappa^2 \Delta^2/2} \right] \\ &= \kappa \left[1 - \frac{(\kappa \Delta)^2}{24} + 0\left((\kappa \Delta)^4\right) \right], \quad \text{for} \quad \left| \frac{(\kappa \Delta)^2}{2} \right| < 1 \; . \end{aligned} \tag{C6}$$

For a multiplying medium, κ and κ' are replaced by iB and iB' respectively, and

$$\begin{aligned} B' &= \frac{1}{\Delta} \tan^{-1} \left[\frac{B \Delta (1 - B^2 \Delta^2/4)^{1/2}}{1 - B^2 \Delta^2/2} \right], \quad \text{for} \quad \left| \frac{(B\Delta)^2}{2} \right| < 1 \\ &= B \left[1 + \frac{(B\Delta)^2}{24} + 0\left((B\Delta)^4\right) \right], \quad \text{for} \quad \left| \frac{(B\Delta)^2}{2 - \sqrt{2}} \right| < 1 \; . \end{aligned} \tag{C7}$$

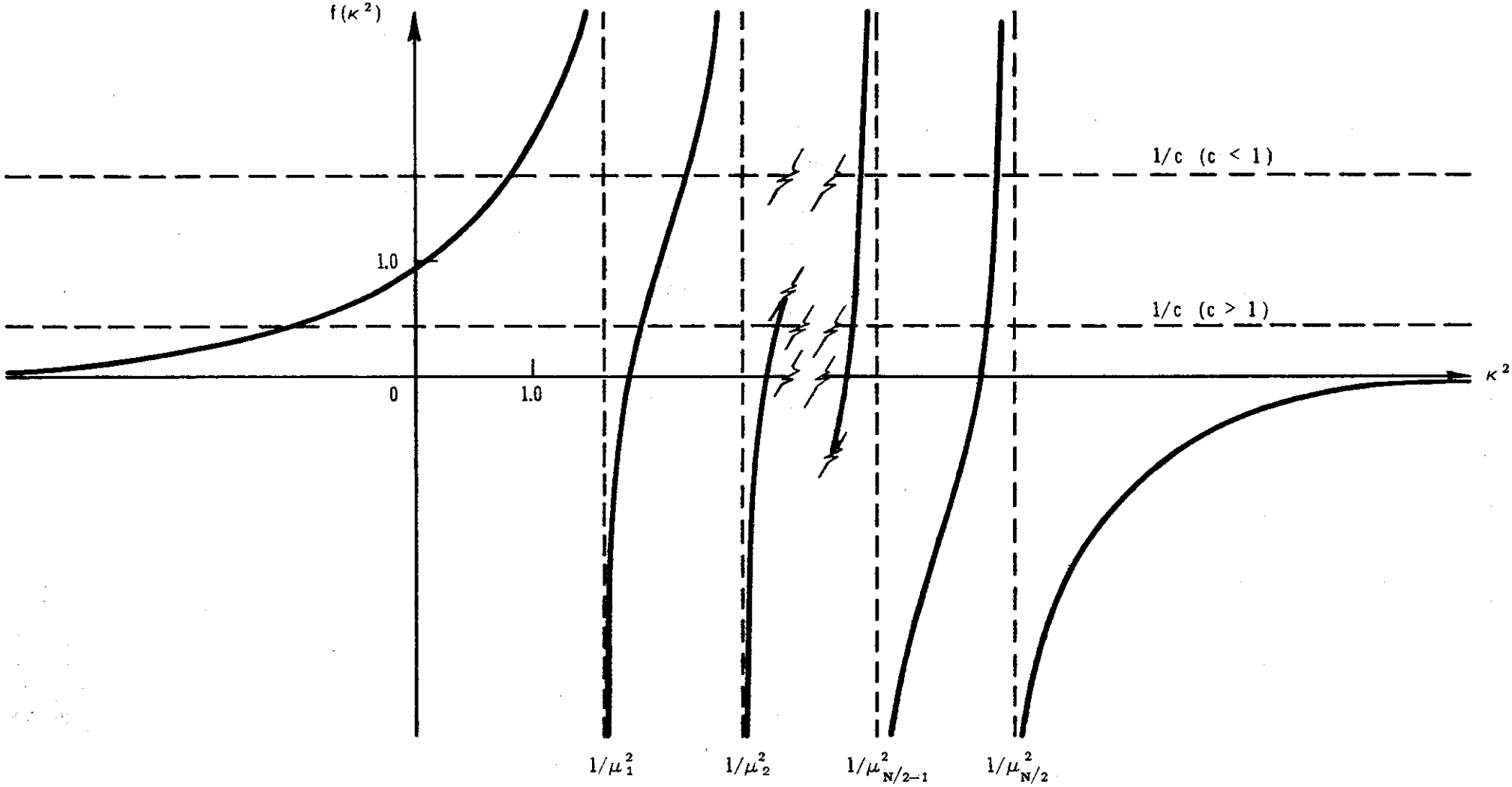

FIGURE 1. THE FUNCTION $f(\kappa^2)$

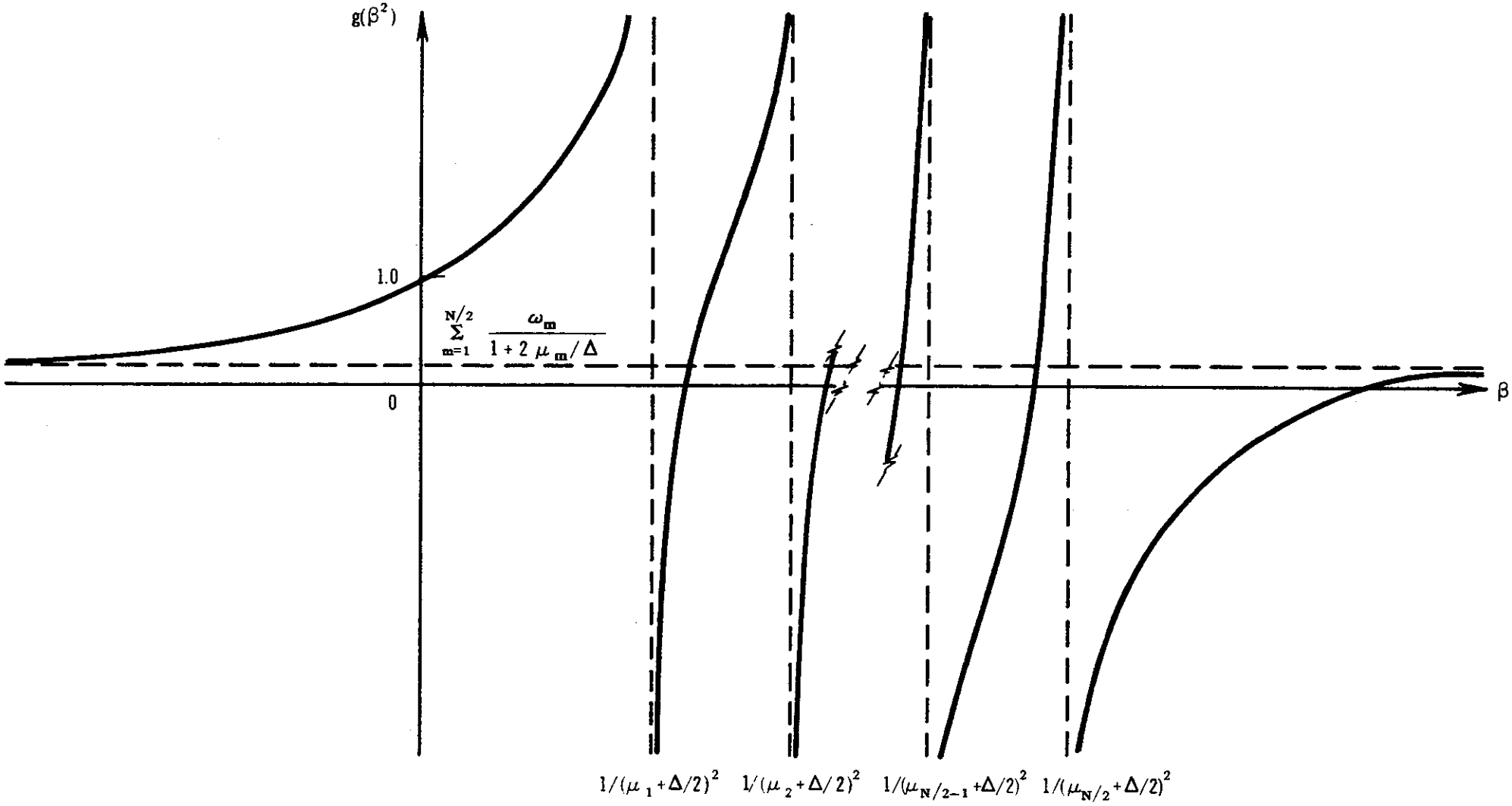

FIGURE 2. THE FUNCTION $g(\beta^2)$